

## Optical microspectroscopy study on enriched (11,10) SWCNTs encapsulating C60 fullerene molecules

Badawi Anis, Kazuhiro Yanagi, Christine A. Kuntscher

### Angaben zur Veröffentlichung / Publication details:

Anis, Badawi, Kazuhiro Yanagi, and Christine A. Kuntscher. 2016. "Optical microspectroscopy study on enriched (11,10) SWCNTs encapsulating C60 fullerene molecules." Carbon 107: 593-99.  
<https://doi.org/10.1016/j.carbon.2016.06.026>.



# Optical microspectroscopy study on enriched (11,10) SWCNTs encapsulating C<sub>60</sub> fullerene molecules

Badawi Anis <sup>a, b</sup>, Kazuhiro Yanagi <sup>c</sup>, C.A. Kuntscher <sup>a, \*</sup>

<sup>a</sup> *Experimentalphysik 2, Universitat Augsburg, 86159 Augsburg, Germany*

<sup>b</sup> *Spectroscopy Department, Physics Division, National Research Centre, 33 El Bohouth St. (former El Tahrir St.), P.O. 12622, Dokki, Giza, Egypt*

<sup>c</sup> *Tokyo Metropolitan University, Hachioji 192-0397, Japan*

## 1. Introduction

Since the discovery of carbon nanotubes (CNTs) in 1991 by Iijima [1], carbon nanotubes stimulate the scientists' curiosity to explore their unusual properties. Single-walled carbon nanotubes (SWCNTs) exhibit exceptional optical, electronic, and mechanical properties, which can be modified by strain, pressure or doping. Their robust mechanical properties are due to the strong sp<sup>2</sup> covalent bonds between the carbon atoms network [2].

As far back as more than fifteen years ago, great achievements have been taken in their synthesis, purification, and explanation of their fundamental physical and chemical properties. Important steps have been taken towards realistic and practical applications of SWCNTs, such as nano-electronics, opto-electronics, energy storage devices, flexible electrodes, nano-composites, and sensors [3]. Therefore, several attempts have been made to tailor their electronic properties, such as chemisorption and physisorption of

atoms on the SWCNTs outer surface, substitution of carbon atoms, intercalation of the nanotubes bundles with atoms or molecules, and filling of the nanotubes' inner cavity [4,5]. Among others, filling is attracting great interest. Due to the tubular structure of SWCNTs, they can be filled with various species: metals, metal halides, organic, organometallic compounds, and other substances [5–8]. With this large variety of different fillers, it is possible to fine tune the electronic and transport properties of SWCNTs [7,8].

For example, C<sub>60</sub> fullerene molecules can be encapsulated in SWCNTs to form a linear chain of fullerene molecules, so-called peapods [9,10]. Encapsulating fullerene and metallofullerene molecules changes the transport properties of the SWCNTs: Scanning tunnelling spectroscopy studies show that the SWCNTs' band gap is modified at the sites where the C<sub>60</sub> fullerene molecules reside [11,12] and the *p*-type SWCNTs field-effect transistor was changed to be ambipolar by encapsulating Gd@C<sub>82</sub> metallofullerene molecules [13]. Therefore, it is particularly important to understand the reaction mechanism between the encapsulated fullerene molecules and the SWCNTs. The encapsulation of the C<sub>60</sub> fullerene molecules in SWCNTs can be discussed in terms of stabilization energy. For SWCNTs with diameter  $d_t < 1.2$  nm the interaction between

\* Corresponding author.

E-mail address: [christine.kuntscher@physik.uni-augsburg.de](mailto:christine.kuntscher@physik.uni-augsburg.de) (C.A. Kuntscher).

nanotubes and  $C_{60}$  molecules is endothermic and the formed peapods system is unstable; whereas the interaction is exothermic for the large SWCNTs diameters  $d \approx 1.2\text{--}1.6$  nm and the formed peapods system is stable [14].

Theoretical studies [15,16] predicted that at a critical tube diameter of  $d_t \geq 1.37$  nm the unoccupied  $t_{1u}$  orbitals of the  $C_{60}$  fullerene molecules hybridize with the nearly free electron state (NFE) of the SWCNTs. The NFE state is located between the nanotube and the  $C_{60}$  molecule and works as an electron acceptor state [15]. Therefore, the hybridization decreases the electronic density in the vicinity of the SWCNTs, and hence the effective tube diameter of the SWCNTs decreases [15–17].

Optical spectroscopy measurements [18–21] on  $C_{60}$ -peapods revealed red and blue shifts of the absorption bands in  $C_{60}$ @SWCNTs peapods ( $\approx \pm 15$  meV) compared to empty SWCNTs with average tube diameter of 1.37–1.5 nm. Also photoluminescence (PL) measurements [22,23] on  $C_{60}$ -peapods over a wide range of diameters ( $\approx 1.22\text{--}1.5$  nm) found a change in the band gap of the SWCNTs with the  $C_{60}$  fullerene filling, where the band gap modifies in a “ $2n+m$ ” family type-dependent manner:  $\Delta E_{11} < 0$  and  $\Delta E_{22} > 0$  for type I  $\text{mod}[(2n+m),3] = 1$  and  $\Delta E_{11} > 0$  and  $\Delta E_{22} < 0$  for type II  $\text{mod}[(2n+m),3] = 2$ . The absorption bands  $E_{ii}$  correspond to the  $i$ th optical transition in the SWCNTs. For SWCNTs with average tube diameter of 1.37–1.5 nm, the maximum change of the band gap was around  $\approx \pm 20$  meV.

All the previous SWCNTs samples used for the preparation of the  $C_{60}$ -peapods were of multi-chirality character, which prevented a detailed understanding of the interaction between the nanotubes and the fullerene molecules. Single chirality SWCNTs have unique electronic properties and diameter. Therefore, they are ideal candidates for the encapsulation of  $C_{60}$  molecules, in order to understand the interaction mechanism between the nanotube and the fullerene molecules. This would potentially open the door to control the chemical and physical properties of SWCNTs, in order to implement such nanostructures in electronic devices.

Here, we report on the preparation of high-yield enriched (11,10) SWCNTs encapsulating  $C_{60}$  fullerene molecules, so called (11,10)-peapods, and also the preparation of DWCNTs derived from the (11,10)-peapods. Raman spectroscopy is used to prove the formation of inner wall inside the (11,10) SWCNT. Optical microspectroscopy is applied to study the effect of the interaction between the fillers ( $C_{60}$  fullerene molecules, inner tube) and the (11,10) SWCNT on the electronic properties.

In general, optical and infrared microspectroscopy is a powerful technique to characterize the electronic band structure in terms of the energy position and spectral weight of the excited interband and intraband transitions. As demonstrated recently, the optical response is capable of monitoring small changes in the electronic band structure of SWCNTs.

## 2. Experimental

The single chirality (11,10) SWCNTs (1.44 nm diameter) were prepared using two purification approaches with Cesium chloride (CsCl) sorting and metal-semiconducting (MS) sorting by usual density-gradient ultracentrifugation. The detailed preparation method is described in Ref. [24] The fraction containing the (11,10) SWCNTs was extracted carefully from the top of the centrifugation tube. Vacuum filtration method was used to prepare bucky-paper from the (11,10) SWCNTs over cellulose nitrate substrate. A small piece of the (11,10) SWCNTs film was transferred in an acetone bath. The free standing film was fished by using a stainless steel substrate with many holes in the middle (see Fig. 1 a–c for illustration).

Bundled multi-chirality SWCNTs were purchased from Carbon Solutions Inc. (Type P2, average diameter 1.4 nm). The P2 carbon

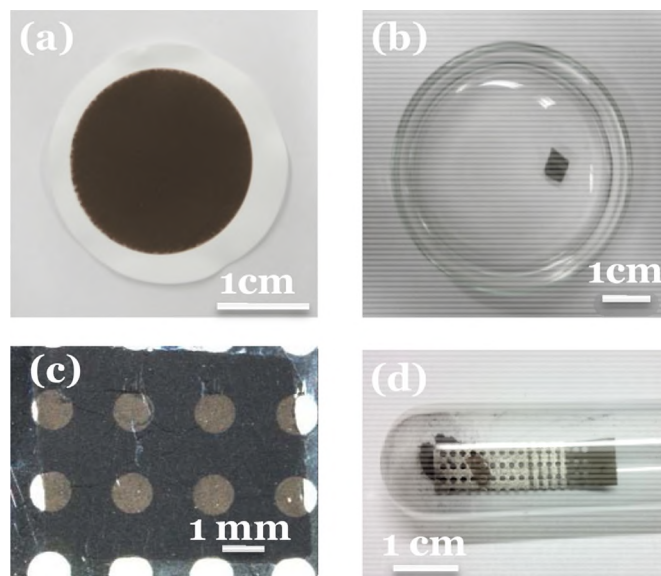


**Fig. 1.** (a) Photograph of the (11,10) SWCNT bucky paper. (b) Free-standing carbon nanotube film floating in acetone solution after dissolution of the cellulose nitrate membrane in the acetone solution. (c) Optical image of the free-standing film over stainless steel substrate. (d) Optical image of the closed evacuated quartz tube containing the (11,10) SWCNT free-standing film over stainless steel substrate and  $C_{60}$  powder. (A colour version of this figure can be viewed online.)

nanotubes were prepared using the arc discharge method. The received P2 carbon nanotubes sample was purified by the supplier to  $>90\%$  carbon content purity. The sample was used without any further purification process. Vacuum filtration was used to prepare bucky-paper multi-chirality SWCNTs over cellulose nitrate substrate from Triton X-100 suspension. The above described procedure (shown in Fig. 1 a–c) has been applied to prepare free-standing films of P2 SWCNTs for optical spectroscopy measurements.

The  $C_{60}$  peapods were prepared by the gas phase method using the (11,10) SWCNT film prepared as described above [19,25]. The typical preparation method is as follows: the caps of the SWCNTs were opened by heating the SWCNTs film over the stainless steel substrate in a furnace at  $575$  °C for 30 min. This process is important to ensure that all the caps are opened and to remove any residuals of amorphous carbon that could be attached to the surface of the SWCNTs. Weighted amount of  $C_{60}$  fullerene powder and the (11,10) SWCNT film were degassed under dynamic vacuum at  $200$  °C for 24 h; after that both samples were sealed in quartz tube under vacuum and heated at  $750$  °C for 5 days continuously (see Fig. 1 d). To remove the non-reacted fullerene molecules from the surface of the (11,10) SWCNTs, the sample was heated at  $700$  °C under dynamic vacuum for 2 h [26,27]. The filling of the (11,10) SWCNT film with  $C_{60}$  molecules enables to measure the change of the optical properties due to the fullerene filling in a quantitative way. Based on our previous work [19,28] and literature data [29,30] on  $C_{60}$  peapods prepared by the gas phase method we can estimate the filling ratio to be higher than 95%.

Transmission data were collected at ambient conditions in the frequency range  $2500\text{--}23,000$   $\text{cm}^{-1}$  using a Bruker IFS 66v/S Fourier transform infrared spectrometer in combination with an infrared microscope (Bruker IR Scope II) with a  $15\times$  magnification objective. The intensity  $I_{\text{sample}}(\omega)$  of the radiation transmitted through the free-standing film and the intensity  $I_{\text{ref}}(\omega)$  of the radiation transmitted through air, as reference, were measured. From  $I_{\text{sample}}(\omega)$  and  $I_{\text{ref}}(\omega)$  the transmittance and absorbance spectra were

calculated according to  $T(\omega) = I_{\text{sample}}(\omega)/I_{\text{ref}}(\omega)$  and  $A(\omega) = -\log_{10} T(\omega)$ , respectively. Room-temperature Raman spectra were measured with a 515 nm excitation line of an argon laser and recorded by a triple Raman spectrometer T64000 (Horiba Jobin Yvon), interfaced to an Olympus BX-40 microscope (100 $\times$  LWD objective). The laser power impinging on the sample was 0.15 mW. The Raman spectrometer was calibrated by using the mercury line at 435.8 nm.

### 3. Results and discussion

The background-subtracted absorbance spectra of (a) (11,10) SWCNTs and (b) multi-chirality SWCNTs free-standing films are depicted in Fig. 2. The absorption bands  $S_{ii}$  and  $M_{ii}$  correspond to the  $i$ th optical transition in the semiconducting and metallic SWCNTs, respectively. The inset of Fig. 2 depicts the raw absorbance spectrum of the free-standing (11,10) SWCNTs film and the absorbance spectrum after the background subtraction. The broad background is due to the  $\pi-\pi^*$  absorption centered at around 5 eV and follows an approximately linear behavior. The absorption bands were fitted with Lorentzian oscillators and the contributions are listed in Table 1. In general, the spectrum of the (11,10) SWCNTs is characterized by three absorptions bands at  $\approx 0.69$ , 1.25, and 2.2–2.4 eV. The  $S_{11}$ ,  $S_{22}$ , and  $S_{33/44}$  bands are due to the first, second, and higher optical transitions in the semiconducting tubes. The absence of significant metallic contributions  $M_{11}$  in the energy range around  $\approx 1.7$  eV signals the semiconducting character of the

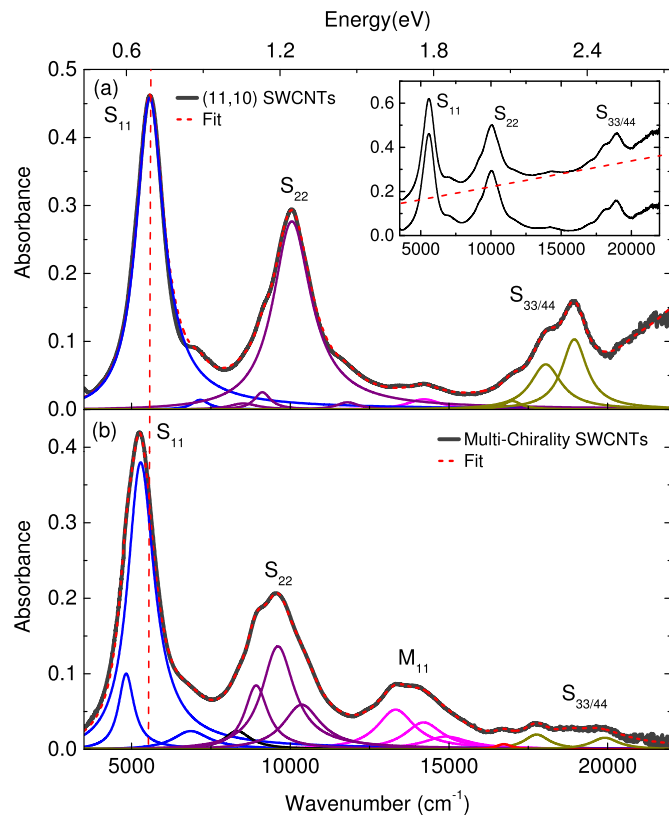


**Fig. 2.** Background-subtracted absorbance spectra of (a) (11,10) SWCNTs and (b) multi-chirality SWCNTs together with the fit of the absorption bands using Lorentzian oscillators. The absorption bands  $S_{ii}$  and  $M_{ii}$  correspond to the  $i$ th optical transition in the semiconducting and metallic SWCNTs, respectively. The vertical, dashed line marks the position of the  $S_{11}$  band in (11,10) SWCNTs. Inset: absorbance spectrum for the (11,10) SWCNTs film together with the linear background (dashed red line) and the absorbance spectrum after background subtraction. (A colour version of this figure can be viewed online.)

**Table 1**

Peak positions in  $\text{cm}^{-1}$  of the Lorentz contributions of the  $S_{11}$ ,  $S_{22}$ ,  $M_{11}$  and  $S_{33/44}$  for SWCNTs, peapods, and DWCNTs.

	$S_{11}$	$S_{22}$	$M_{11}$	$S_{33/44}$
Multi-chirality SWCNTs	4800	8960	13,300	17,763
	5255	9610	14,180	18,873
	6920	10,330	15,098	19,909
(11,10) SWCNTs	5575	10,050		16,996
				18,050
				18,950
Multi-chirality Peapods	4866	9020	13,440	16,875
	5350	9676	14,260	17,911
	6940	10,340	15,120	18,947
(11,10) Peapods	5114	9676		20,257
				17,474
				18,405
(11,10) DWCNTs	5327	9720		17,584
				18,460

sample. The  $S_{11}$  and  $S_{22}$  absorption bands can be described by one strong Lorentzian oscillator respectively, which reflects the single-chirality nature of the sample. The small Lorentzian contributions close to the  $S_{22}$  absorption bands indicate a small amount of other chiralities besides (11,10) SWCNTs.

In comparison, the background-subtracted absorbance spectrum of the multi-chirality SWCNTs free-standing film is shown in Fig. 2 (b). The fine structure of the  $S_{11}$ ,  $S_{22}$ ,  $M_{11}$ , and  $S_{33/44}$  bands reflects the rather large diameter and chirality distribution in the sample. The absorption bands were fitted with Lorentzian oscillators and the contributions are listed in Table 1. Our previous work [19,31] showed that the P2-SWCNTs have a diameter distribution from 1.3 to 1.5 nm with an average tube diameter of 1.42 nm.

It is clear from Table 1 that the  $S_{11}$ ,  $S_{22}$ , and  $S_{33/44}$  absorption bands in the multi-chirality SWCNTs free-standing film are redshifted compared to the (11,10) SWCNTs. This red shift could be attributed to the bundling effect, as explained in the following. The multi-chirality SWCNTs free-standing film was prepared by sonicating the P2-SWCNTs powder in a Triton X-100 solution, then the solution was left over night to allow the large bundles to settle down. The clear supernatant solution was filtered over a cellulose nitrate film. However, in the case of the (11,10) SWCNTs, before the chirality separation the SWCNTs powder was dispersed into a 2% (w/w) sodium cholate (SC) and 42.5% (w/w) CsCl solution by using tip homogenizer for 4 h, then the solution was centrifuged for 1 h at 40,000 rpm. The SWCNTs supernatant was used for the single-chirality separation. It has been shown that the sonication and centrifugation of bundled SWCNTs decrease the bundling to a limiting value associated with individually dispersed SWCNTs [32]. This means that the degree of bundling in the case of the multi-chirality SWCNTs free-standing film is higher than that in the case of the (11,10) SWCNTs free-standing film. Previous theoretical and experimental studies [33,34] showed that the bundling effect leads to a lowering of the symmetry of individual SWCNTs in a bundle. Therefore, the separation between the valence and the conduction band is reduced, resulting in a red shift of tens of meV in the optical absorption bands.

To clarify the effect of the  $C_{60}$  filling on the optical properties of the (11,10) SWCNTs, we plot in Fig. 3 the background-subtracted absorbance spectrum of (a) (11,10) peapods and (b) multi-chirality peapods free-standing films. The absorption bands were fitted with Lorentzian oscillators, and the contributions are listed in Table 1.

Compared to the empty (11,10) SWCNTs [Fig. 2 (a)] one observes that all absorption bands in the (11,10) peapods are redshifted ( $\approx 60$  meV for  $S_{11}$ , 50 meV for  $S_{22}$ , and 67–70 meV for  $S_{33/44}$ ), broadened, and lost spectral weight. See also Fig. 5 for a direct

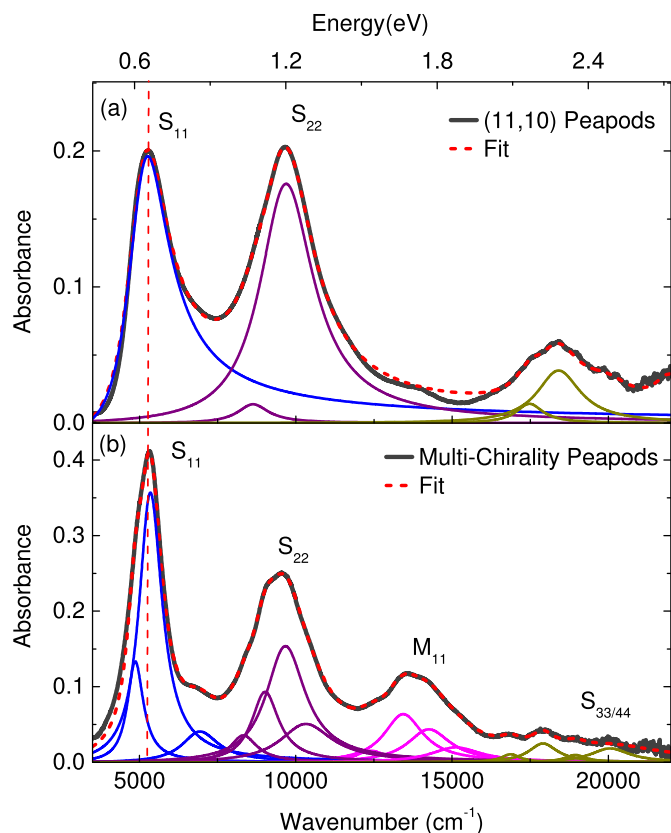


**Fig. 3.** Background-subtracted absorbance spectra of (a) (11,10) peapods and (b) multi-chirality peapods together with the fit of the absorption bands using Lorentzian oscillators. The absorption bands  $S_{ii}$  and  $M_{ii}$  correspond to the  $i$ th optical transition in the semiconducting and metallic SWCNTs, respectively. The vertical, dashed line marks the position of the  $S_{11}$  band in (11,10) peapods. (A colour version of this figure can be viewed online.)

comparison between the results for (11,10) SWCNTs and (11,10) peapods. When compared to literature data, this behavior is not expected for our peapods system. For the multi-chirality peapods, no obvious changes in the spectrum in comparison to multi-chirality SWCNTs [Fig. 2 (b)] are found, except for the slight blue shift in the energy position of the absorption bands [see Table 1]. According to our previous work [19] on multi-chirality peapods, the blue shift of the absorption bands can be attributed to the hybridization between the NFE state of the SWCNTs and the  $t_{1u}$  state of the  $C_{60}$ , since hybridization is expected to reduce the effective tube diameter [15,16], and hence the optical absorption bands are blue-shifted according to the Kataura plot [35].

Now we will discuss the optical properties of (11,10) peapods as compared to empty (11,10) SWCNTs. In general, the redshift, broadening, and loss of spectral weight of the optical absorption bands could be attributed to strain-induced effects, the hybridization between the  $t_{1u}$  orbitals of the  $C_{60}$  molecules and the NFE states of the SWCNTs [22,23] or the symmetry breaking of the nanotubes [28,31,36,37]. The band gap modification upon insertion of  $C_{60}$  molecules was found to be diameter- and chirality-dependent [22,23]. The band gap related to the first and the second optical transitions,  $E_{11}$  and  $E_{22}$ , respectively, even changes in opposite direction between type I and type II SWCNTs due to strain-induced effects [22,23]. For example, strain/hybridization leads to a redshift of 66 meV for  $E_{22}$  and a blue shift of 12 meV for  $E_{11}$  in (13,5) SWCNTs (type I), whereas for the (15,2) SWCNTs (type II) a redshift of 60 meV for  $E_{11}$  and a blue shift of 32 meV for  $E_{22}$  were found. For

larger diameters ( $d_t \geq 1.3$  nm), the shifts in energy position of the optical transitions  $E_{11}$  and  $E_{22}$  approach zero and change their sign [22,23]. A photoluminescence study by Okubo et al. [22] showed that the induced changes in the  $S_{11}$  and  $S_{22}$  transitions is zero in (11,10) SWCNTs encapsulating  $C_{60}$  fullerene molecules. Therefore, hybridization between the electronic states in (11,10) SWCNTs and the  $C_{60}$  molecules cannot be considered as the primary reason for the observed large redshift of the optical absorption bands. Neither can they be related to strain-induced effects, since theoretical calculations [15,16] predict that these do not occur for diameters  $d_t \geq 1.3$  nm (the diameter of (11,10) SWCNTs is 1.44 nm).

A theoretical study on the energetic and the mechanical stability of  $C_{60}$  peapods using density-functional theory (DFT), molecular mechanics, and molecular dynamics simulations [38,39] showed that the interaction between the  $C_{60}$  fullerene molecules and the nanotube wall strongly depends on the space between them. For (10,10) SWCNTs the inter-space amounts to 3.325 Å, which is very close to the graphite interlayer space (3.35 Å) [40]. Therefore, homogeneous attractive van der Waals (vdW) interactions between the  $C_{60}$  fullerene molecules and the nanotube wall from both sides are to be expected, leading to a homogeneous arrangement of the  $C_{60}$  molecules in the center of the nanotube. As the nanotube diameter increases, the inter-space between  $C_{60}$  molecules and the nanotube wall increases and the vdW attraction will be one-sided. Meaning that the encapsulation of the fullerene molecules will enhance the deformation of the nanotubes for larger diameter than the (10,10) SWCNTs [38]. In the case of (11,10) peapods, the inter-space between the SWCNTs and the  $C_{60}$  molecules amounts to 3.67 Å, which is, however, still close to the graphite interlayer space. Therefore, the redshift and loss of spectral weight of the absorption bands cannot be attributed due to the non-homogenous interactions between the  $C_{60}$  molecules and the nanotube wall.

It is important to note that the optical excitations in carbon nanotubes cannot be explained in terms of simple single electron interband transitions. The optical excitations are found to be of excitonic nature [30], and hence their energetic position is a combination of the band gap energy and the exciton binding energy [30,41]. It has been furthermore shown that the dielectric environment affects the optical excitation energies in carbon nanotubes [42–47].

As the dielectric constant increases, the Coulomb interactions (electron-hole) and the self-energy (electron-electron repulsion) are screened. The decrease of the self-energy always exceeds the exciton binding energy, which results in an overall redshift of the optical transitions [46–48]. The redshift is consistent with the theoretical calculations [47–51] and experimental results [46,52]. A maximum redshift of  $55 \pm 4$  meV for  $E_{11}$  and  $50 \pm 10$  meV for  $E_{22}$  was observed. The redshifts saturate at an environmental dielectric constant of  $\sim 5$ , without any significant (n,m) dependence [46,48,52].

Furthermore, theoretical calculations by Miyauchi et al. [47] demonstrated that the screening effect is related to the static dielectric constant  $\epsilon$  as a linear combination of both the dielectric constant of the surrounding environment  $\epsilon_{env}$  and the internal environment, which is called the dielectric constant of the nanotube itself,  $\epsilon_{tube}$ . Hence, the dielectric constant  $\epsilon$  is calculated according to the equation:

$$\frac{1}{\epsilon} = \frac{C_{env}}{\epsilon_{env}} + \frac{C_{tube}}{\epsilon_{tube}} \quad (1)$$

where  $C_{env}$  and  $C_{tube}$  are coefficients for the outside and inside of a nanotube, respectively [47]. Here, the nanotube and its surrounding medium are considered as a series connection of two capacitors with different dielectric constants where the electric flux lines pass

through the two dielectric materials. The constants  $C_{env}$  and  $C_{tube}$  are dimensional constants, i.e., their values depend on the nanotube diameter [47], therefore both values will not change after the filling. In our studies the optical properties of the (11,10) SWCNTs and (11,10) peapods free-standing films were measured in air, i.e.,  $\epsilon_{env} \approx 1$ . Accordingly, the dielectric screening will depend only on the internal dielectric constant of the nanotube  $\epsilon_{tube}$ , which is affected by the filling. Assuming the dielectric constant of the encapsulated  $C_{60}$  fullerene molecules to be 4–4.5 [53,54], we attribute the observed redshift of the optical absorption bands in the case of the (11,10) peapods as compared to (11,10) SWCNTs to an increase of the internal dielectric constant  $\epsilon_{tube}$  of the nanotubes after filling.

The decrease in spectral weight of the  $S_{11}$  and  $S_{22}$  absorption bands in (11,10) peapods compared to empty SWCNTs could be attributed to the charge transfer from the nanotubes to the fullerene molecules. Theoretical [55] and experimental [20] studies showed that electrons are transferred from SWCNTs to  $C_{60}$  molecules. Therefore,  $C_{60}$  molecules are considered as a hole dopant [20,55–57]. It has been shown that [58,59] the p-doping reduces the electron density in the semiconducting SWCNTs and lowers the Fermi level into the valence band toward the first van Hove singularity or below, and hence the  $S_{11}$  and  $S_{22}$  absorption bands are partially quenched [60].

In order to test the above stated assumptions regarding the effect of the internal dielectric constant and the charge transfer between the nanotubes and the  $C_{60}$  molecules, the same free-standing (11,10) peapods film was transformed to DWCNTs using the laser irradiation method [61,62]. Here, we aim to change both the internal dielectric constant and the charge transfer between the nanotubes and the  $C_{60}$  molecules. The sample was irradiated with 514 nm laser (250 mW) for 5 min under high vacuum. The activation barrier for the  $C_{60}$  molecules polymerization was found to be 1.4 eV [38] indicating that the 514 nm (2.4 eV) is suitable to overcome the activation barrier. We also tried the thermal transformation of the (11,10) peapods to DWCNTs under dynamic vacuum (at 1200 °C for 24 h), but it was not possible in this case. As shown in Fig. 1 (d) the free-standing film is very small (1 mm<sup>2</sup>) and fragile, therefore the dynamic vacuum with the very high temperature destroyed the nanotube film. After laser irradiation a small piece of the (11,10) DWCNTs free-standing film and of the (11,10) SWCNT film were transferred on a SiO<sub>2</sub> substrate for Raman measurements.

The inset of Fig. 4 depicts the Raman spectrum of the empty (11,10) SWCNTs, before filling, as a reference. The spectrum was fitted with Lorentzian functions, in order to specify the various contributions. The obtained peak positions are given in the spectrum. Accordingly, we observe the radial breathing mode (RBM) of the outer tubes at 173 cm<sup>-1</sup>. The small shoulder at 183.3 cm<sup>-1</sup> could be attributed to a different chirality present in the (11,10) SWCNTs sample. The diameter  $d$  of the (11,10) SWCNTs was calculated according to the relation  $\omega_{RBM} = 248/d$  and amounts to  $d \approx 1.43$  nm (This formula is used for carbon nanotubes dispersed on SiO<sub>2</sub> substrate) [63]. The obtained value matches that of the diameter of the (11,10) SWCNTs [24].

Fig. 4 shows the Raman spectrum of the (11,10) DWCNTs including the fit with Lorentzian functions. For the (11,10) DWCNTs, the RBM of the outer tube is observed at 166.6 cm<sup>-1</sup>. The small shoulder observed at 176.3 cm<sup>-1</sup> is attributed to a different chirality present in the starting (11,10) SWCNTs sample. At higher frequencies, one can observe a peak at 363.3 cm<sup>-1</sup> with quite low intensity in addition to some weak contributions close to this peak. In contrast, in the case of (11,10) SWCNTs (see the inset of Fig. 4) no Raman features are observed for the empty tubes. In general the Raman modes detected in this frequency range (300–400 cm<sup>-1</sup>) for

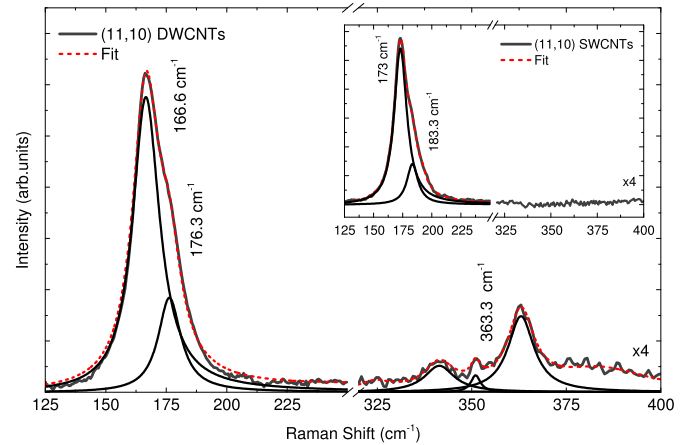


**Fig. 4.** Raman spectrum recorded with a 515 nm excitation wavelength showing the RBMs for (11,10) DWCNTs. Modes in the range 300–400 cm<sup>-1</sup> correspond to the RBMs of the inner tubes. Raman spectra in the range 300–400 cm<sup>-1</sup> were multiplied by a factor of 4. The dashed-red line is a fit to the data with Lorentzian functions. The Lorentz contributions are shown as well. Inset: Raman spectrum recorded with 532 nm excitation wavelength showing the RBMs of the empty (11,10) SWCNTs together with a fit with Lorentzian functions. (A colour version of this figure can be viewed online.)

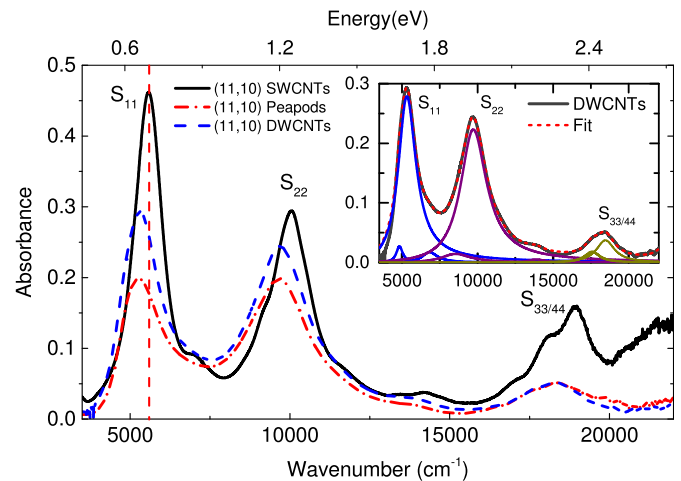


**Fig. 5.** Background-subtracted absorbance spectra of (11,10) SWCNTs, (11,10) peapods, and (11,10) DWCNTs together with the fit of the absorption bands using Lorentzian oscillators. The absorption bands  $S_{ij}$  corresponds to the  $i$ th optical transition in the semiconducting SWCNTs. The vertical, dashed line marks the position of the  $S_{11}$  band in (11,10) SWCNTs. Inset: Absorbance spectrum for the (11,10) DWCNTs film together with the fit of the absorption bands using Lorentzian oscillators. (A colour version of this figure can be viewed online.)

DWCNTs derived from  $C_{60}$  peapods are associated with the RBMs of the inner tubes [27,64]. According to the Kataura plot [35] the 2.4 eV excitation energy matches well with the outer tubes via the energy spacing  $S_{33}$ . On the other hand, the 2.4 eV energy is unsuitable for resonant enhancement of inner tubes; only the smaller inner tubes with diameter  $\sim 0.7$ – $0.8$  nm are resonant with this excitation energy via the energy spacing  $S_{22}$ . Therefore, the observed quite low intensity of the RBM of the inner tubes is expected with the 2.4 eV laser excitation [65,31]. The inner diameter  $d$  of the (11,10) DWCNTs was calculated according to the above relation and amounts to  $d \approx 0.68$  nm. The obtained value for  $d$  is very close to the diameter of the  $C_{60}$  fullerene molecules.

The background-subtracted absorbance spectrum of the (11,10) DWCNTs free-standing film is plotted in Fig. 5 in comparison with

(11,10) SWCNTs and (11,10) peapods. The absorption bands were fitted with Lorentzian oscillators (see the inset of Fig. 5) and the contributions are listed in Table 1. One finds that the absorption bands of the (11,10) DWCNTs are red shifted ( $\approx 30$  meV for  $S_{11}$ , 40 meV for  $S_{22}$ , and 57–60 meV for  $S_{33/44}$ ) compared to the (11,10) SWCNTs, but blue shifted (by  $\approx 30$  meV for  $S_{11}$ , 10 meV for  $S_{22}$ , and 10–13 meV for  $S_{33/44}$ ) compared to the (11,10) peapods. The blue shift of the absorption bands in the case of (11,10) DWCNTs compared to (11,10) peapods could be attributed to the decrease of the internal dielectric constant. The dielectric constant of SWCNTs is  $\sim 3.2$  [66] which is less than the dielectric constant of the  $C_{60}$  molecules. Furthermore, from Fig. 5 one can see that the spectral weight of the (11,10) DWCNTs absorption bands is increased compared to the (11,10) peapods, but it is still less than that found for the empty (11,10) SWCNTs. Theoretical [67] and experimental [5,68] studies on the charge transfer between the outer and inner tubes in DWCNTs demonstrated that electrons are transferred from the outer wall to the inner one. Therefore, the decrease of the spectral weight of the  $S_{11}$  and  $S_{22}$  compared to the empty tubes is related to the charge transfer from the outer to the inner tube, and hence electrons are removed from the van Hove singularities in the occupied density of states in the outer tube.

From the above discussion we can conclude that the (11,10) SWCNTs provide a clean environment for studying the interaction between the  $C_{60}$  molecules and the nanotubes. In contrast, the absorption bands in multi-chirality SWCNTs are much more complicated, and a precise identification of their modifications with filling is difficult.

#### 4. Conclusion

In conclusion, the interaction between  $C_{60}$  fullerene molecules and (11,10) SWCNTs has been characterized in terms of the optical transitions. For (11,10) SWCNTs, the observation of three strong  $S_{11}$ ,  $S_{22}$ , and  $S_{33/44}$  absorption bands with the absence of  $M_{11}$  metallic contributions reflects the clean and well-defined environment of the (11,10) SWCNTs for studying the interaction between the  $C_{60}$  molecules and the nanotubes. The absorption bands of the multi-chirality SWCNTs are red-shifted compared to the (11,10) SWCNTs. This red shift could be attributed to the bundling effect in the multi-chirality SWCNTs. Compared to the empty (11,10) SWCNTs, the optical absorption bands for the (11,10) peapods show a redshift ( $\approx 60$  meV for  $S_{11}$ , 50 meV for  $S_{22}$ , and 67–70 meV for  $S_{33/44}$ ) and spectral weight reduction in the case of the  $S_{11}$  and  $S_{22}$  absorption bands. This redshift is explained in terms of an increase of the internal dielectric constant in peapods compared to empty nanotubes. The reduction of the spectral weight of the  $S_{11}$  absorption band is attributed to the electron transfer from the (11,10) SWCNTs to the encapsulated  $C_{60}$  molecules. This idea is supported by the transformation of the (11,10) peapods to DWCNTs by the laser irradiation method. The formation of the DWCNTs was confirmed by Raman spectroscopy. The inner tubes' diameters in the DWCNTs amounts to  $\approx 0.68$  nm, as derived from the RBM frequencies. The transformation of the fullerene molecules to an inner tube partially reduces the internal dielectric constant and the charge transfer.

#### Acknowledgement

We acknowledge financial support by the DFG (KU 1432/3-2).

#### References

- [1] S. Iijima, Helical microtubules of graphitic carbon, *Nature* 354 (6348) (1991) 56–58, <http://dx.doi.org/10.1038/354056a0>.
- [2] A. Jorio, R. Saito, G. Dresselhaus, M.S. Dresselhaus, *Raman Spectroscopy in Graphene Related Systems*, Wiley-VCH Verlag, Weinheim, 2011, <http://dx.doi.org/10.1002/9783527632695.fmatter>.
- [3] C.H. Liu, H.L. Zhang, Chemical approaches towards single-species single-walled carbon nanotubes, *Nanoscale* 2 (2010) 1901–1918, <http://dx.doi.org/10.1039/C0NR00306A>.
- [4] D. Tasis, N. Tagmatarchis, A. Bianco, M. Prato, *Chemistry of carbon nanotubes*, *Chem. Rev.* 106 (3) (2006) 1105–1136, <http://dx.doi.org/10.1021/cr050569o>.
- [5] M.V. Kharlamova, M. Sauer, T. Saito, Y. Sato, K. Suenaga, T. Pichler, et al., Doping of single-walled carbon nanotubes controlled via chemical transformation of encapsulated nickelocene, *Nanoscale* 7 (2015) 1383–1391, <http://dx.doi.org/10.1039/c4nr05586a>.
- [6] M. Kharlamova, Novel approach to tailoring the electronic properties of single-walled carbon nanotubes by the encapsulation of high-melting gallium selenide using a single-step process, *JETP Lett.* 98 (5) (2013) 272–277, <http://dx.doi.org/10.1134/S0021364013180069>.
- [7] T. Okazaki, H. Shinohara, Nano-peapods encapsulating fullerenes, in: S. Rotkin, S. Subramoney (Eds.), *Applied Physics of Carbon Nanotubes*. NanoScience and Technology, Springer Berlin, Heidelberg, 2005, ISBN 978-3-540-23110-3, pp. 133–150.
- [8] D.A. Britz, A.N. Khlobystov, Noncovalent interactions of molecules with single walled carbon nanotubes, *Chem. Soc. Rev.* 35 (2006) 637–659, <http://dx.doi.org/10.1039/B507451G>.
- [9] B.W. Smith, M. Monthieux, D.E. Luzzi, Encapsulated  $C_{60}$  in carbon nanotubes, *Nature* 396 (1998) 323–324, <http://dx.doi.org/10.1038/24521>.
- [10] B.W. Smith, M. Monthieux, D.E. Luzzi, Carbon nanotube encapsulated fullerenes: a unique class of hybrid materials, *Chem. Phys. Lett.* 315 (12) (1999) 31–36, [http://dx.doi.org/10.1016/S0009-2614\(99\)00896-9](http://dx.doi.org/10.1016/S0009-2614(99)00896-9).
- [11] D.J. Hornbaker, S.J. Kahng, S. Misra, B.W. Smith, A.T. Johnson, E.J. Mele, et al., Mapping the one-dimensional electronic states of nanotube peapod structures, *Science* 295 (5556) (2002) 828–831, <http://dx.doi.org/10.1126/science.1068133>.
- [12] J. Lee, H. Kim, S.J. Kahng, G. Kim, Y.W. Son, J. Ihm, et al., Bandgap modulation of carbon nanotubes by encapsulated metallofullerenes, *Nature* 415 (6875) (2002) 1005–1008, <http://dx.doi.org/10.1038/4151005a>.
- [13] T. Shimada, T. Okazaki, R. Taniguchi, T. Sugai, H. Shinohara, K. Suenaga, et al., Ambipolar field-effect transistor behavior of  $Gd@C_{60}$  metallofullerene peapods, *Appl. Phys. Lett.* 81 (21) (2002) 4067–4069, <http://dx.doi.org/10.1063/1.1522482>.
- [14] A. Rochefort, Electronic and transport properties of carbon nanotube peapods, *Phys. Rev. B* 67 (2003) 115401, <http://dx.doi.org/10.1103/PhysRevB.67.115401>.
- [15] S. Okada, S. Saito, A. Oshiyama, Energetics and electronic structures of encapsulated  $C_{60}$  in a carbon nanotube, *Phys. Rev. Lett.* 86 (2001) 3835–3838, <http://dx.doi.org/10.1103/PhysRevLett.86.3835>.
- [16] M. Otani, S. Okada, A. Oshiyama, Energetics and electronic structures of one-dimensional fullerene chains encapsulated in zigzag nanotubes, *Phys. Rev. B* 68 (2003) 125424, <http://dx.doi.org/10.1103/PhysRevB.68.125424>.
- [17] S. Okada, Radial-breathing mode frequencies for nanotubes encapsulating fullerenes, *Chem. Phys. Lett.* 438 (13) (2007) 59–62, <http://dx.doi.org/10.1016/j.cplett.2007.02.058>.
- [18] A. Ryabenko, N. Kiselev, J. Hutchison, T. Moroz, S. Bukalov, L. Mikhailitsyn, et al., Spectral properties of single-walled carbon nanotubes encapsulating fullerenes, *Carbon* 45 (7) (2007) 1492–1505, <http://dx.doi.org/10.1016/j.carbon.2007.03.031>.
- [19] B. Anis, M. Fischer, M. Schreck, K. Haubner, L. Dunsch, C.A. Kuntscher, Synthesis and characterization of peapods and dwcnts, *Phys. Status Solidi (B)* 249 (12) (2012) 2345–2348, <http://dx.doi.org/10.1002/pssb.201200096>.
- [20] X. Liu, T. Pichler, M. Knupfer, M.S. Golden, J. Fink, H. Kataura, et al., Filling factors, structural, and electronic properties of  $C_{60}$  molecules in single-wall carbon nanotubes, *Phys. Rev. B* 65 (2002) 045419, <http://dx.doi.org/10.1103/PhysRevB.65.045419>.
- [21] S.K. Joung, T. Okazaki, S. Okada, S. Iijima, Interaction between single-wall carbon nanotubes and encapsulated  $C_{60}$  probed by resonance raman spectroscopy, *Phys. Chem. Chem. Phys.* 12 (2010) 8119–8123, <http://dx.doi.org/10.1039/C000102C>.
- [22] S. Okubo, T. Okazaki, N. Kishi, S.K. Joung, T. Nakanishi, S. Okada, et al., Diameter-dependent band gap modification of single-walled carbon nanotubes by encapsulated fullerenes, *J. Phys. Chem. C* 113 (2) (2009) 571–575, <http://dx.doi.org/10.1021/jp807630z>.
- [23] T. Okazaki, S. Okubo, T. Nakanishi, S.K. Joung, T. Saito, M. Otani, et al., Optical band gap modification of single-walled carbon nanotubes by encapsulated fullerenes, *J. Am. Chem. Soc.* 130 (12) (2008) 4122–4128, <http://dx.doi.org/10.1021/ja711103y>.
- [24] M. Kawai, H. Kyakuno, T. Suzuki, T. Igarashi, H. Suzuki, T. Okazaki, et al., Single chirality extraction of single-wall carbon nanotubes for the encapsulation of organic molecules, *J. Am. Chem. Soc.* 134 (23) (2012) 9545–9548, <http://dx.doi.org/10.1021/ja3013853>.
- [25] K. Hirahara, K. Suenaga, S. Bandow, H. Kato, T. Okazaki, H. Shinohara, et al., One-dimensional metallofullerene crystal generated inside single-walled carbon nanotubes, *Phys. Rev. Lett.* 85 (2000) 5384–5387, <http://dx.doi.org/10.1103/PhysRevLett.85.5384>.
- [26] F. Simon, H. Peterlik, R. Pfeiffer, J. Bernardi, H. Kuzmany, Fullerene release from the inside of carbon nanotubes: a possible route toward drug delivery, *Chem. Phys. Lett.* 445 (46) (2007) 288–292, <http://dx.doi.org/10.1016/>

- j.cplett.2007.08.014.
- [27] S. Bandow, M. Takizawa, K. Hirahara, M. Yudasaka, S. Iijima, Raman scattering study of double-wall carbon nanotubes derived from the chains of fullerenes in single-wall carbon nanotubes, *Chem. Phys. Lett.* 337 (13) (2001) 48–54, [http://dx.doi.org/10.1016/S0009-2614\(01\)00192-0](http://dx.doi.org/10.1016/S0009-2614(01)00192-0).
- [28] B. Anis, F. Börrnert, M.H. Rummeli, C.A. Kuntscher, High-pressure optical microspectroscopy study on single-walled carbon nanotubes encapsulating C<sub>60</sub>, *J. Phys. Chem. C* 117 (42) (2013) 21995–22001, <http://dx.doi.org/10.1021/jp405639t>.
- [29] R. Pfeiffer, C. Kramberger, C. Schaman, A. Sen, M. Holzweber, H. Kuzmany, et al., Defect free inner tubes in dwncts, *AIP Conf. Proc.* 685 (1) (2003) 297–301, <http://dx.doi.org/10.1063/1.1628038>.
- [30] F. Simon, M. Monthioux, Fullerenes inside carbon nanotubes: the peapods, in: M. Monthioux (Ed.), *Carbon Meta-nanotubes: Synthesis, Properties and Applications*, John Wiley & Sons, Ltd, 2012, pp. 273–321, <http://dx.doi.org/10.1002/9781119954743.ch5b> chap. 5b.
- [31] B. Anis, F. Börrnert, M.H. Rummeli, C.A. Kuntscher, Optical microspectroscopy study of the mechanical stability of empty and filled carbon nanotubes under hydrostatic pressure, *J. Phys. Chem. C* 118 (46) (2014) 27048–27062, <http://dx.doi.org/10.1021/jp506922s>.
- [32] J.F. Cardenas, A. Gromov, The effect of bundling on the g' Raman band of single-walled carbon nanotubes, *Nanotechnology* 20 (46) (2009) 465703, <http://dx.doi.org/10.1088/0957-4484/20/46/465703>.
- [33] S. Reich, C. Thomsen, P. Ordejón, Electronic band structure of isolated and bundled carbon nanotubes, *Phys. Rev. B* 65 (2002) 155411, <http://dx.doi.org/10.1103/PhysRevB.65.155411>.
- [34] F. Wang, M.Y. Sfeir, L. Huang, X.M.H. Huang, Y. Wu, J. Kim, et al., Interactions between individual carbon nanotubes studied by Rayleigh scattering spectroscopy, *Phys. Rev. Lett.* 96 (2006) 167401, <http://dx.doi.org/10.1103/PhysRevLett.96.167401>.
- [35] H. Kataura, Y. Kumazawa, Y. Maniwa, I. Umezumi, S. Suzuki, Y. Ohtsuka, et al., Optical properties of single-wall carbon nanotubes, *Synth. Met.* 103 (13) (1999) 2555–2558, [http://dx.doi.org/10.1016/S0379-6779\(98\)00278-1](http://dx.doi.org/10.1016/S0379-6779(98)00278-1).
- [36] J. Strauch, B. Anis, C.A. Kuntscher, High-pressure optical study of bromine-doped single-walled carbon nanotube films, *Phys. Status Solidi (B)* 251 (12) (2014) 2378–2383, <http://dx.doi.org/10.1002/pssb.201451160>.
- [37] B. Anis, K. Haubner, F. Börrnert, L. Dunsch, M.H. Rummeli, C.A. Kuntscher, Stabilization of carbon nanotubes by filling with inner tubes: an optical spectroscopy study on double-walled carbon nanotubes under hydrostatic pressure, *Phys. Rev. B* 86 (2012) 155454, <http://dx.doi.org/10.1103/PhysRevB.86.155454>.
- [38] S. Okada, Energetics of carbon peapods: elliptical deformation of nanotubes and aggregation of encapsulated C<sub>60</sub>, *Phys. Rev. B* 77 (2008) 235419, <http://dx.doi.org/10.1103/PhysRevB.77.235419>.
- [39] C.c. Ling, Q.z. Xue, D. Xia, M.x. Shan, Z.d. Han, Fullerene filling modulates carbon nanotube radial elasticity and resistance to high pressure, *RSC Adv.* 4 (2014) 1107–1115, <http://dx.doi.org/10.1039/C3RA45594G>.
- [40] Y. Baskin, L. Meyer, Lattice constants of graphite at low temperatures, *Phys. Rev.* 100 (1955) 544, <http://dx.doi.org/10.1103/PhysRev.100.544>, 544.
- [41] R. Saito, M.S. Dresselhaus, Optical properties of carbon nanotubes, in: K.T. Iijima (Ed.), *Carbon Nanotubes and Graphene*, second ed., Elsevier, Oxford, 2014, pp. 77–98, <http://dx.doi.org/10.1016/B978-0-08-098232-8.00005-X> chap. 5.
- [42] Y. Ohno, S. Iwasaki, Y. Murakami, S. Kishimoto, S. Maruyama, T. Mizutani, Chirality-dependent environmental effects in photoluminescence of single-walled carbon nanotubes, *Phys. Rev. B* 73 (2006) 235427, <http://dx.doi.org/10.1103/PhysRevB.73.235427>.
- [43] S. Chou, H. Ribeiro, E. Barros, A. Santos, D. Nezhich, G. Samsonidze, et al., Optical characterization of dna-wrapped carbon nanotube hybrids, *Chem. Phys. Lett.* 397 (46) (2004) 296–301, <http://dx.doi.org/10.1016/j.cplett.2004.08.117>.
- [44] V.C. Moore, M.S. Strano, E.H. Haroz, R.H. Hauge, R.E. Smalley, J. Schmidt, et al., Individually suspended single-walled carbon nanotubes in various surfactants, *Nano Lett.* 3 (10) (2003) 1379–1382, <http://dx.doi.org/10.1021/nl034524j>.
- [45] C. Fantini, A. Jorio, M. Souza, M.S. Strano, M.S. Dresselhaus, M.A. Pimenta, Optical transition energies for carbon nanotubes from resonant Raman spectroscopy: environment and temperature effects, *Phys. Rev. Lett.* 93 (2004) 147406, <http://dx.doi.org/10.1103/PhysRevLett.93.147406>.
- [46] Y. Ohno, S. Iwasaki, Y. Murakami, S. Kishimoto, S. Maruyama, T. Mizutani, Excitonic transition energies in single-walled carbon nanotubes: dependence on environmental dielectric constant, *Phys. Status Solidi (B)* 244 (11) (2007) 4002–4005, <http://dx.doi.org/10.1002/pssb.200776124>.
- [47] Y. Miyauchi, R. Saito, K. Sato, Y. Ohno, S. Iwasaki, T. Mizutani, et al., Dependence of exciton transition energy of single-walled carbon nanotubes on surrounding dielectric materials, *Chem. Phys. Lett.* 442 (46) (2007) 394–399, <http://dx.doi.org/10.1016/j.cplett.2007.06.018>.
- [48] J. Jiang, R. Saito, G.G. Samsonidze, A. Jorio, S.G. Chou, G. Dresselhaus, et al., Chirality dependence of exciton effects in single-wall carbon nanotubes: tight-binding model, *Phys. Rev. B* 75 (2007) 035407, <http://dx.doi.org/10.1103/PhysRevB.75.035407>.
- [49] T. Ando, Theory of electronic states and transport in carbon nanotubes, *J. Phys. Soc. Jpn.* 74 (3) (2005) 777–817, <http://dx.doi.org/10.1143/JPSJ.74.777>.
- [50] V. Perebeinos, J. Tersoff, P. Avouris, Scaling of excitons in carbon nanotubes, *Phys. Rev. Lett.* 92 (2004) 257402, <http://dx.doi.org/10.1103/PhysRevLett.92.257402>.
- [51] A.R.T. Nugraha, R. Saito, K. Sato, P.T. Araujo, A. Jorio, M.S. Dresselhaus, Dielectric constant model for environmental effects on the exciton energies of single wall carbon nanotubes, *Appl. Phys. Lett.* 97 (9) (2010) 091905, <http://dx.doi.org/10.1063/1.3485293>.
- [52] O.A. Dyatlova, J. Gomis-Bresco, E. Malic, H. Telg, J. Maultzsch, G. Zhong, et al., Dielectric screening effects on transition energies in aligned carbon nanotubes, *Phys. Rev. B* 85 (2012) 245449, <http://dx.doi.org/10.1103/PhysRevB.85.245449>.
- [53] D.L. Perry (Ed.), *Inorganic Compound Data*, second ed., CRC Press, USA, 2011.
- [54] M. Dresselhaus, G. Dresselhaus, P. Eklund, Crystalline structure of fullerene solids, in: M.D.D. Eklund (Ed.), *Science of Fullerenes and Carbon Nanotubes*, Academic Press, San Diego, 1996, pp. 171–223, <http://dx.doi.org/10.1016/B978-01221820-0/50007-1>.
- [55] V. Prudkovskiy, M. Berd, E. Pavlenko, K. Katin, M. Maslov, P. Puech, et al., Electronic coupling in fullerene-doped semiconducting carbon nanotubes probed by Raman spectroscopy and electronic transport, *Carbon* 57 (2013) 498–506, <http://dx.doi.org/10.1016/j.carbon.2013.02.027>.
- [56] M.V. Kharlamova, Advances in tailoring the electronic properties of single-walled carbon nanotubes, *Prog. Mater. Sci.* 77 (2016) 125–211, <http://dx.doi.org/10.1016/j.pmatsci.2015.09.001>.
- [57] C.A. Reed, R.D. Bolskar, Discrete fulleride anions and fullerene cations, *Chem. Rev.* 100 (3) (2000) 1075–1120, <http://dx.doi.org/10.1021/cr980017o>.
- [58] J.L. Blackburn, T.M. Barnes, M.C. Beard, Y.H. Kim, R.C. Tenent, T.J. McDonald, et al., Transparent conductive single-walled carbon nanotube networks with precisely tunable ratios of semiconducting and metallic nanotubes, *ACS Nano* 2 (6) (2008) 1266–1274, <http://dx.doi.org/10.1021/nm800200d>.
- [59] K.S. Mistry, B.A. Larsen, J.D. Bergeson, T.M. Barnes, G. Teeter, C. Engtrakul, et al., n-type transparent conducting films of small molecule and polymer amine doped single-walled carbon nanotubes, *ACS Nano* 5 (5) (2011) 3714–3723, <http://dx.doi.org/10.1021/nn200076r>.
- [60] D.W. Shin, J.H. Lee, Y.H. Kim, S.M. Yu, S.Y. Park, J.B. Yoo, A role of hno3 on transparent conducting film with single-walled carbon nanotubes, *Nanotechnology* 20 (47) (2009) 475703, <http://dx.doi.org/10.1088/0957-4484/20/47/475703>.
- [61] C. Kramberger, A. Waske, K. Biedermann, T. Pichler, T. Gemming, B. Bchner, et al., Tailoring carbon nanostructures via temperature and laser irradiation, *Chem. Phys. Lett.* 407 (46) (2005) 254–259, <http://dx.doi.org/10.1016/j.cplett.2005.03.089>.
- [62] M. Berd, P. Puech, A. Righi, A. Benfdila, M. Monthioux, Resonant laser-induced formation of double-walled carbon nanotubes from peapods under ambient conditions, *Small* 8 (13) (2012) 2045–2052, <http://dx.doi.org/10.1002/sml.201102410>.
- [63] S. Ping Han, A. William, I. Goddard, Coupling of raman radial breathing modes in double-wall carbon nanotubes and bundles of nanotubes, *J. Phys. Chem. B* 113 (20) (2009) 7199–7204, <http://dx.doi.org/10.1021/jp805828g>.
- [64] S. Bandow, G. Chen, G.U. Sumanasekera, R. Gupta, M. Yudasaka, S. Iijima, et al., Diameter-selective resonant raman scattering in double-wall carbon nanotubes, *Phys. Rev. B* 66 (2002) 075416, <http://dx.doi.org/10.1103/PhysRevB.66.075416>.
- [65] R. Pfeiffer, F. Simon, H. Kuzmany, V.N. Popov, Fine structure of the radial breathing mode of double-wall carbon nanotubes, *Phys. Rev. B* 72 (2005) 161404, <http://dx.doi.org/10.1103/PhysRevB.72.161404>.
- [66] E. Sano, E. Akiba, Electromagnetic absorbing materials using nonwoven fabrics coated with multi-walled carbon nanotubes, *Carbon* 78 (2014) 463–468, <http://dx.doi.org/10.1016/j.carbon.2014.07.027>.
- [67] V. Zólyomi, J. Koltai, A. Ruzsnyák, J. Kürti, A. Gali, F. Simon, et al., Intershell interaction in double walled carbon nanotubes: charge transfer and orbital mixing, *Phys. Rev. B* 77 (2008) 245403, <http://dx.doi.org/10.1103/PhysRevB.77.245403>.
- [68] H. Shiozawa, T. Pichler, C. Kramberger, A. Grüneis, M. Knupfer, B. Büchner, et al., Fine tuning the charge transfer in carbon nanotubes via the interconversion of encapsulated molecules, *Phys. Rev. B* 77 (2008) 153402, <http://dx.doi.org/10.1103/PhysRevB.77.153402>.